



UNIVERSITY OF LEEDS

This is a repository copy of *Quantitative assessment of colorectal morphology: Implications for robotic colonoscopy*.

White Rose Research Online URL for this paper:
<http://eprints.whiterose.ac.uk/96558/>

Version: Accepted Version

Article:

Alazmani, A, Hood, A, Jayne, D et al. (2 more authors) (2016) Quantitative assessment of colorectal morphology: Implications for robotic colonoscopy. *Medical Engineering & Physics*, 38 (2). pp. 148-154. ISSN 1350-4533

<https://doi.org/10.1016/j.medengphy.2015.11.018>

© 2016, Elsevier. Licensed under the Creative Commons Attribution-NonCommercial-NoDerivatives 4.0 International
<http://creativecommons.org/licenses/by-nc-nd/4.0/>

Reuse

Unless indicated otherwise, fulltext items are protected by copyright with all rights reserved. The copyright exception in section 29 of the Copyright, Designs and Patents Act 1988 allows the making of a single copy solely for the purpose of non-commercial research or private study within the limits of fair dealing. The publisher or other rights-holder may allow further reproduction and re-use of this version - refer to the White Rose Research Online record for this item. Where records identify the publisher as the copyright holder, users can verify any specific terms of use on the publisher's website.

Takedown

If you consider content in White Rose Research Online to be in breach of UK law, please notify us by emailing eprints@whiterose.ac.uk including the URL of the record and the reason for the withdrawal request.



eprints@whiterose.ac.uk
<https://eprints.whiterose.ac.uk/>

Quantitative Assessment of Colorectal Morphology: Implications for Robotic Colonoscopy

A. Alazmani^{*1}, A. Hood², D. Jayne², A. Neville¹, and P. Culmer³

¹ Institute of Functional Surfaces (iFS), School of Mechanical Engineering, University of Leeds, Woodhouse Lane, Leeds, LS2 9JT, UK

² Academic Surgical Unit, St. James's University Hospital, Leeds Leeds, LS9 7TF, UK

³ Institute of Engineering Systems and Design, School of Mechanical Engineering, University of Leeds, Woodhouse Lane, Leeds, LS2 9JT, UK

[Corresponding Author]

Ali Alazmani

Address:

Institute of Functional Surfaces (iFS)
School of Mechanical Engineering,
University of Leeds,
Leeds, LS2 9JT
UK

Tel: +44 (0)113 343 2106

Fax: +44 (0)113 242 4611

Email: a.alazmani@leeds.ac.uk

Abstract

This paper presents a method of characterizing the distribution of colorectal morphometrics. It uses three-dimensional region growing and topological thinning algorithms to determine and visualize the luminal volume and centerline of the colon, respectively. Total and segmental lengths, diameters, volumes, and tortuosity angles were then quantified. The effects of body orientations on these parameters were also examined. Variations in total length were predominately due to differences in the transverse colon and sigmoid segments, and did not significantly differ between body orientations. The diameter of the proximal colon was significantly larger than the distal colon, with the largest value at the ascending and caecum segments. The volume of the transverse colon was significantly the largest, while those of the descending colon and rectum were the smallest. The prone position showed a higher frequency of high angles and consequently found to be more torturous than the supine position. This study yielded a method for complete segmental measurements of healthy colorectal anatomy and its tortuosity. The transverse and sigmoid colons were the major determinant in tortuosity and morphometrics between body orientations. Quantitative understanding of these parameters may potentially help to facilitate colonoscopy techniques, accuracy of polyp spatial distribution detection, and design of novel endoscopic devices.

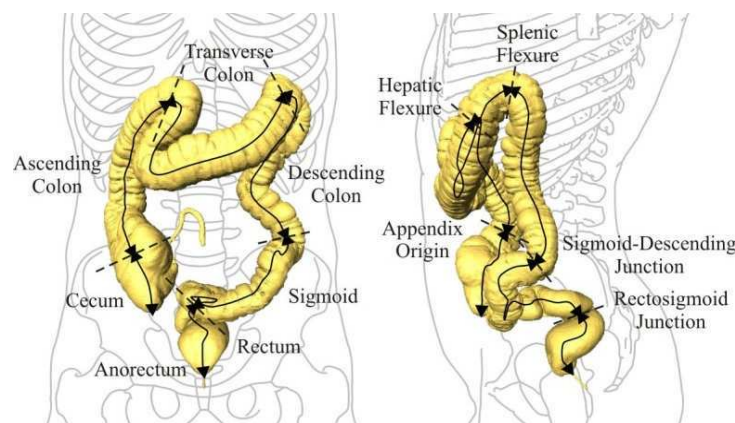
Keywords: Robotic Colonoscopy, Colon, Large Intestine, Colorectal Cancer

47 1 Introduction

48 Colorectal cancer (CRC) is the third most common cancer worldwide, estimated to cause 10.2%
 49 and 12.7% of the total cancer death in the UK and USA respectively [1, 2]. Currently, video-
 50 colonoscopy is the preferred screening method for the diagnosis of CRC [3, 4], however, it is attended
 51 by certain clinical drawbacks such as patient discomfort, need for sedation, absence of
 52 maneuverability of the scope, and a long learning curve. In order to improve compliance to the
 53 screening programs, an imaging modality - computed tomographic colonography (CTC) - was
 54 developed for early detection of colorectal polyps and cancer [5]. Other new technologies are being
 55 evaluated and have started to emerge, e.g. computer assisted colonoscopy [6-10] and active capsule
 56 colonoscopy [11-13]. Similar to conventional colonoscopy, endoluminal navigation in these new
 57 technologies is often challenging due to the convoluted nature of the colon.

58 Although the colon anatomy is well described, less is known about the variation of colorectal
 59 morphometry in quantitative terms across the general population. Studies have shown that colonic
 60 anatomical features have a significant association with failure to achieve complete colonoscopy [14].
 61 An understanding of the length, diameter and tortuosity of the colon is important for the performance
 62 of conventional colonoscopy; and specially for the future development of robotic colonoscopy
 63 platforms that may have sections of fixed diameter and length. Consequently, using this information,
 64 important features such as colonic elongation and distension can be extracted, and statistical
 65 assessments such as polyp spatial distribution can be understood.

66 Colonic length has been investigated previously using barium enema, where accurate length
 67 assessment is difficult due to the three-dimensional (3-D) intraluminal centreline. Only one study was
 68 found from the barium enema literature where the colonic diameter was estimated, in this case for
 69 Japanese men and women [15]. It is of note that in these studies the colon contains a significant
 70 volume of barium which may also influence the accuracy of measurements. Several barium enema
 71 and intraoperative laparotomy studies have investigated how various colonic parameters and gender
 72 might predict the degree of difficulty during colonoscopic examinations [16-18], but did not aim to
 73 determine the morphology and tortuosity of the colon. One study described the intestinal length as a
 74 whole in cadavers did not provide the length of the colonic segments used clinically [19]. Fig. 1
 75 shows the 3-D geometry of the lumen and its anatomical segments. Several CTC studies reported the
 76 length measurements for the colorectal anatomy [20, 21] and its correlation with difficult or
 77 incomplete examinations [22, 23]. The high resolution of CTC technology, combined with regular
 78 CO₂ insufflation and automated digital analyses, make this technology a far more accurate tool for
 79 assessing the anatomy of the colon when compared to other methods such as barium enema. However,
 80 little is known about the complete colon length, intra-colon segmental lengths, diameters, volume, and
 81 tortuosity angle of colorectal anatomy in a healthy population.



82
 83 Fig. 1. Schematic representation of the colonic segments and landmarks in anterior and lateral views; the
 84 dashed line represents the anatomical landmark position. All measurements were recorded for the six segments
 85 (rectum, sigmoid, descending, transverse, ascending, and cecum) using the automated centreline along the axis
 86 of the colonic lumen, solid arrow lines.

87 The aim of our investigation was to describe a method to quantitatively measure the luminal
 88 length, diameter, volume, and shape of the colon within an asymptomatic population undergoing

89 primary CTC examinations. We also determined whether a correlation exists between these factors,
90 and between scans taken in supine and prone orientations. These descriptors may have implications
91 for conventional colonoscopy and CT colonography training and performance. Furthermore, they
92 provide a quantitative description of the colonic environment that can be used for development of new
93 colonoscopy devices, from incremental advances to current colonoscope technology to next-
94 generation robotic systems [24]. An understanding of the diameter and tortuosity of the colon is
95 particularly relevant for the future of these systems.

96 **2 Materials and Methods**

97 **2.1 Patient Preparation and Data Acquisition**

98 A single medically qualified researcher, under supervision of a consultant radiologist, searched the publically
99 available TCIA (<http://cancerimagingarchive.net/>, sponsored by the Cancer Imaging Program, DCTD/NCI/NIH)
100 retrospectively and selected clinical studies that demonstrated reportedly healthy colons in both prone and
101 supine positions (no patients were excluded from this population). In total, 24 patient studies were selected at
102 random: 12 men and 12 women. The average age of the sample was 54.8 ± 4.7 years ranging from 50 to 65.

103 The complete imaging methodology has been described previously [25]. Briefly, all patients had undergone
104 standard 24-hour colonic preparation with stool tagging following by the oral administration of 90 mL of
105 sodium phosphate (Phospho-soda, Fleet Pharmaceuticals) and bisacodyl tablets (10 mg) to reduce the presence
106 of any residual stool or fluid. The final step was to ingest a 6-oz (177 mL) glass of liquid containing at least 5
107 mL and up to 60 mL of water-soluble iodinated oral contrast material (diatrizoate meglumine and sodium
108 diatrizoate, Gastroview, Mallinckrodt Imaging) the night before the examination to label any residual colonic
109 fluid. All examinations were performed using at least a 16-channel helical CT scanner with 0.8 mm collimation,
110 1 mm reconstruction interval, matrix 512×512, 50 effective mAs, peak voltage of 120 kV, and B30f convolution
111 kernel. Data were obtained in the supine and prone positions; 1 mg of glucagon was administered
112 subcutaneously 7–15 minutes before the CT examination unless contraindicated or refused by the patient.
113 Colonic distention was achieved with an automated carbon dioxide insufflator (PROTOCO2L, E-Z-EM).

114 **2.2 Image Segmentation and Centerline**

115 We developed a multistage algorithm to process the CT data and generate a 3-D volumetric polygon mesh,
116 with an associated centerline, to be used in a quantitative description of the colon morphology. The first stage
117 employs clinical visualization software (Amira, FRI Visualization Sciences Group, USA) to identify low
118 attenuation voxels that represent gas in the colon lumen using a 3-D region growing algorithm [26]. An intensity
119 based threshold of less than -800HU was experimentally determined for each dataset (grey-level histogram of
120 the abdominal CT dataset) to segment the lumen's details. Increasing this threshold allows more details of the
121 lumen interior to be visualized, however, too high threshold may result in erroneous inclusion of the
122 surrounding tissue. Because the colon is not the only gas-filled organ, user-defined seed points were placed in
123 the lumen to spatially isolate the colon. If the value of the connected voxels were less than the intensity
124 threshold, they were included in the region. This algorithm stopped when no more voxels remain in the collected
125 neighbors. Two datasets required additional user interaction to guide the algorithm due to lumen occlusion by
126 peristalsis, spasm and/or residual faeces. This modeling was then checked against a visual review of the images
127 to ensure accuracy.

128 The segmented data was resampled to produce regular pixel spacing. The visualization software was then
129 used to implement a topological thinning algorithm to obtain a skeleton representation of the segmented colon
130 lumen. Using the anorectum as the starting point and most distal part of the cecum as the end point, the
131 algorithm automatically performs a skeleton tracing of the colon. The two endpoints required for centerline
132 calculation can also be automatically identified during the segmentation process based on distance fields [27].
133 Due to the complexity of the segmented colonic lumen (e.g., haustral folds), the resulting skeleton may contain
134 many paths between two endpoints when only one corresponds to the centerline of the colon. We used a graph
135 theoretic algorithm, described by Ge *et al.*, to remove extra branches [28] which are typically anomalies close to
136 the surface of the colon lumen rather than features associated with the actual centerline. The skeleton then
137 becomes a single **continuous line from rectum** to cecum, positioned centrally in the colon lumen and termed
138 herein the 'centreline'.

139 **2.3 Anatomical Colorectal Landmarks**

140 As depicted in Fig. 1, the 3-D geometry of the lumen was classified into 6 anatomical segments using

landmarks identified on the centerline; the rectum, sigmoid colon, descending colon, transverse colon, ascending colon, and cecum [29]. The spatial coordinates of these landmarks were evaluated by the same expert researcher. The rectosigmoid junction was located between the sacral promontory and the S3 vertebral body levels and included in the sigmoid colon. The pelvic brim was chosen as the location for sigmoid-descending junction which the distal descending colon angles forwards. The leftmost and rightmost, most cranial inflexion points of the colon were designated as the descending-transverse and transverse-ascending junctions, respectively (the splenic and hepatic flexures). The ileocaecal valve was selected as a boundary between the ascending colon and the cecum, where the valve was included in the proximal segment. The colon was also divided into two functional parts: the proximal colon from the most proximal part of the cecum to the splenic flexure; and the distal colon, from the splenic flexure to the anorectum.

2.4 Data Processing

The final stage of processing was performed using a custom program (implemented in Matlab, Mathworks Inc., USA) to analyze the 3-D volume and associated centerline of the colon for each dataset and from these compute the morphological metrics. To minimize local fluctuations in the centerline, the path was linearly resampled at regular 1 mm intervals along its length and then smoothed with a 40 point moving average filter.

Colorectal length and volume were calculated from the 3-D volume of the colon lumen and its centerline between the successive colonic landmarks shown in Fig. 1. The effective colonic cross-section was described using a circle-fitting approach. This was done as the cross-section of the colonic lumen can have functionally redundant areas. Firstly, a series of planes were defined normal to each component of the centerline (between successive 1 mm points) and then the intersection of this plane with the colonic 3-D volume was found. This yielded a set of planar points for each cross-sectional plane. An iterative circle-fitting algorithm was then implemented to determine the radius of the largest circle which fits inside this point set, using the centerline point as an initial estimate for the circle's center since it will always lie within the lumen. Collating these data then provides the effective radius at 1 mm intervals along the colon's length.

Although the tortuosity does not have a formal clinical definition, there are clearly some intuitive properties, which a reasonable index must satisfy in order for it to correlate with the gross qualitative assessment of an expert observer. In order to obtain a meaningful tortuosity measure for the engineering community, we have calculated the in-plane angle of the centerline using a span size equal to the total mean diameter of the lumen (~ 3.5 cm), as shown in Fig. 2.

3 Results

We analyzed the colonic morphology in 24 patients in both supine and prone positions using the method described above. The variations in colonic elongation and tortuosity are visualized in Fig. 3. All the measurements were compared using the Wilcoxon signed-rank test and then underwent further post-hoc analysis using Exact testing to allow for the small number of subjects used with the significant level set at 0.05 ($p < 0.05$). Table 1-3 summarize the length, diameter and volume of each colonic segment and proximal, distal, and the total colons. The z-value is the test statistic for Wilcoxon signed-rank testing.

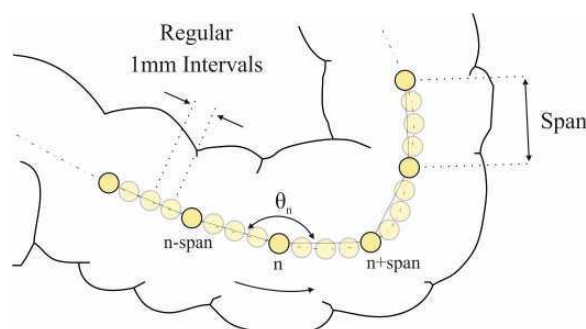


Fig. 2. Methodology for determining the angle (θ) of each point on the colonic centreline (e.g., at point n , this angle was calculated by measuring the angle formed by two vectors between $(n) \rightarrow (n\text{-span})$ and $(n) \rightarrow (n\text{+span})$).

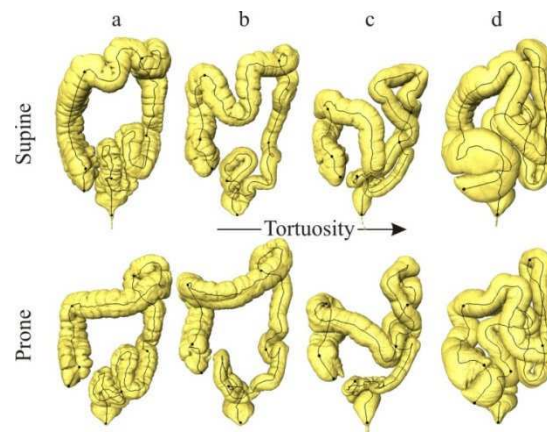


Fig. 3. 3-D visualisation of the segmented colonic volumes from CTC, images are from patients TCIA 26, 87, 179, and 62. These cases demonstrate how colonic elongation and tortuosity (specifically for transverse and sigmoid segments) differ from a relatively short textbook colon (a) to an elongated and tortuous colon (d). The automated centreline is overlaid on the rendered colons that allow morphometric measurements.

There was no significant difference in total colonic length between the supine (185.0 ± 18.3 cm) and prone (183.0 ± 16.9 cm), nor was there any significant differences when mean lengths between men and women groups were compared (187.7 ± 19.0 cm in men and 182.2 ± 18.1 cm in women). However, when the colonic segments were considered, significant differences were found during positional. The descending colon was found to be significantly shorter in the supine position ($z = -2.171$, $p < 0.03$), while the ascending colon and cecum significantly shorter in the prone orientation. The length of the transverse colon and sigmoid colon were significantly the largest in both orientations, followed by the descending colon, rectum, ascending colon, and caecum. The transverse and sigmoid segments also demonstrated the widest length variation in both positions. When considering the proximal and distal lengths of the colon, the distal colon was found to be longer in both orientations. The sigmoid colon was significantly longer (supine: $p < 0.038$ and prone: $p < 0.04$) in women (supine: 54.4 ± 10.8 cm and prone: 53.5 ± 11.2 cm) than in men (supine: 46.8 ± 15.9 cm and prone: 46.4 ± 11.6 cm). The descending and ascending colons were significantly longer in both directions in men ($p < 0.001$). The cecum length was longer in male, but this finding attained significance only in the prone position ($p < 0.001$). The length of the other segments did not significantly differ between the two gender groups.

The cross-sectional properties of the colon were considered across the entire colon length and per-segment. Fig. 4 shows a frequency distribution of colorectal radius across the group. Supine and prone orientations exhibit similar trends, although the supine data are more positively skewed towards higher radii. Fig. 5, Fig. 6 and Table 2 provide further detail of the radius within each segment of the colon. The mean diameter of the ascending colon (supine: 4.5 cm and prone: 4.3 cm) was the largest followed by that of the cecum (supine: 4.4 cm and prone: 3.8 cm) in both orientations. The diameter of the sigmoid colon was significantly the smallest (2.6 cm in both orientations) being the longest and narrowest segment of the colon. The diameter of the proximal colon was significantly larger than the distal colon in both supine and prone orientations.

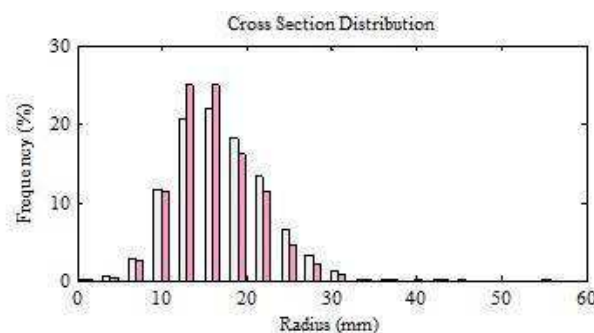


Fig. 4. Radius distribution for 24 patients in supine (white columns) and prone (pink columns) orientations

218

219 Table 1. Comparison of the colonic segmental Length in supine and prone orientations in 24 patients
 220 (mean \pm SD (median))

	Length, cm		
	Supine	<i>z</i> -value (<i>p</i>)	Prone
Rectum	23.4 \pm 6.7 (21.7)	-0.400 (0.705)	23.1 \pm 3.9 (22.7)
Sigmoid	50.6 \pm 13.9 (51.6)	-0.971 (0.345)	49.9 \pm 11.7 (48.7)
Descending	24.2 \pm 7.8 (23.1)	-2.171 (0.029*)	26.0 \pm 7.8 (25.9)
Transverse	57.2 \pm 9.3 (56.6)	-0.086 (0.944)	57.3 \pm 10.9 (56.9)
Ascending	21.7 \pm 4.2 (20.7)	-2.114 (0.034*)	19.7 \pm 4.0 (20.3)
Cecum	7.8 \pm 2.9 (6.9)	-2.029 (0.042*)	6.9 \pm 2.3 (6.8)
Proximal	86.6 \pm 9.7 (85.5)	-2.086 (0.037*)	84.0 \pm 10.2 (82.9)
Distal	98.3 \pm 14.7 (97.7)	-0.057 (0.966)	99.0 \pm 11.8 (98.8)
Total Colon	185.0 \pm 18.3 (187.5)	-1.086 (0.290)	183.0 \pm 16.9 (185.0)

221 * Statistically Significant

222

223 Table 2. Comparison of the colonic segmental diameter in supine and prone orientations in 24
 224 patients (mean \pm SD (median))

	Diameter, cm		
	Supine	<i>z</i> -value (<i>p</i>)	Prone
Rectum	3.6 \pm 0.8 (3.4)	-1.400 (0.166)	3.7 \pm 0.7 (3.6)
Sigmoid	2.6 \pm 0.4 (2.5)	-1.263 (0.214)	2.6 \pm 0.3 (2.6)
Descending	3.3 \pm 0.6 (3.3)	-1.072 (0.294)	3.2 \pm 0.5 (3.1)
Transverse	3.7 \pm 0.4 (3.7)	-2.030 (0.042*)	3.6 \pm 0.5 (3.5)
Ascending	4.5 \pm 0.7 (4.7)	-2.359 (0.017*)	4.3 \pm 0.7 (4.6)
Cecum	4.4 \pm 0.7 (4.5)	-3.187 (0.001*)	3.8 \pm 0.6 (3.9)
Proximal	4.2 \pm 0.4 (4.3)	-3.514 (0.000*)	3.9 \pm 0.5 (4.0)
Distal	3.1 \pm 0.5 (3.0)	-4.286 (0.000*)	3.1 \pm 0.4 (3.1)
Total Colon	4.7 \pm 0.5 (4.7)	-4.286 (0.000*)	3.5 \pm 0.4 (3.5)

225 * Statistically Significant

226

227 Table 3. Comparison of the colonic segmental volume in supine and prone orientations in 24 patients
 228 (mean \pm SD (median))

	Volume, cm ³		
	Supine	<i>z</i> -value (<i>p</i>)	Prone
Rectum	154.4 \pm 49.3 (156.7)	-1.686 (0.095*)	170.1 \pm 44.0 (166.2)
Sigmoid	195.6 \pm 104.9 (165.5)	-0.686 (0.509)	190.2 \pm 92.2 (156.7)
Descending	159.2 \pm 78.1 (154.8)	-1.057 (0.303)	168.7 \pm 79.7 (165.3)
Transverse	477.9 \pm 147.9 (466.9)	-1.429 (0.160)	454.7 \pm 150.1 (433.2)
Ascending	233.6 \pm 92.0 (237.0)	-2.914 (0.003*)	198.0 \pm 94.9 (201.4)
Cecum	156.1 \pm 370.3 (64.2)	-2.229 (0.025*)	57.8 \pm 28.6 (57.2)
Proximal	867.6 \pm 483.7 (823.0)	-2.943 (0.002*)	710.5 \pm 212.0 (706.6)
Distal	509.2 \pm 181.7 (448.2)	-0.857 (0.406)	529.0 \pm 166.7 (481.7)
Total Colon	1376.8 \pm 582.4 (1267.9)	-1.829 (0.069)	1239.5 \pm 344.0 (1164.5)

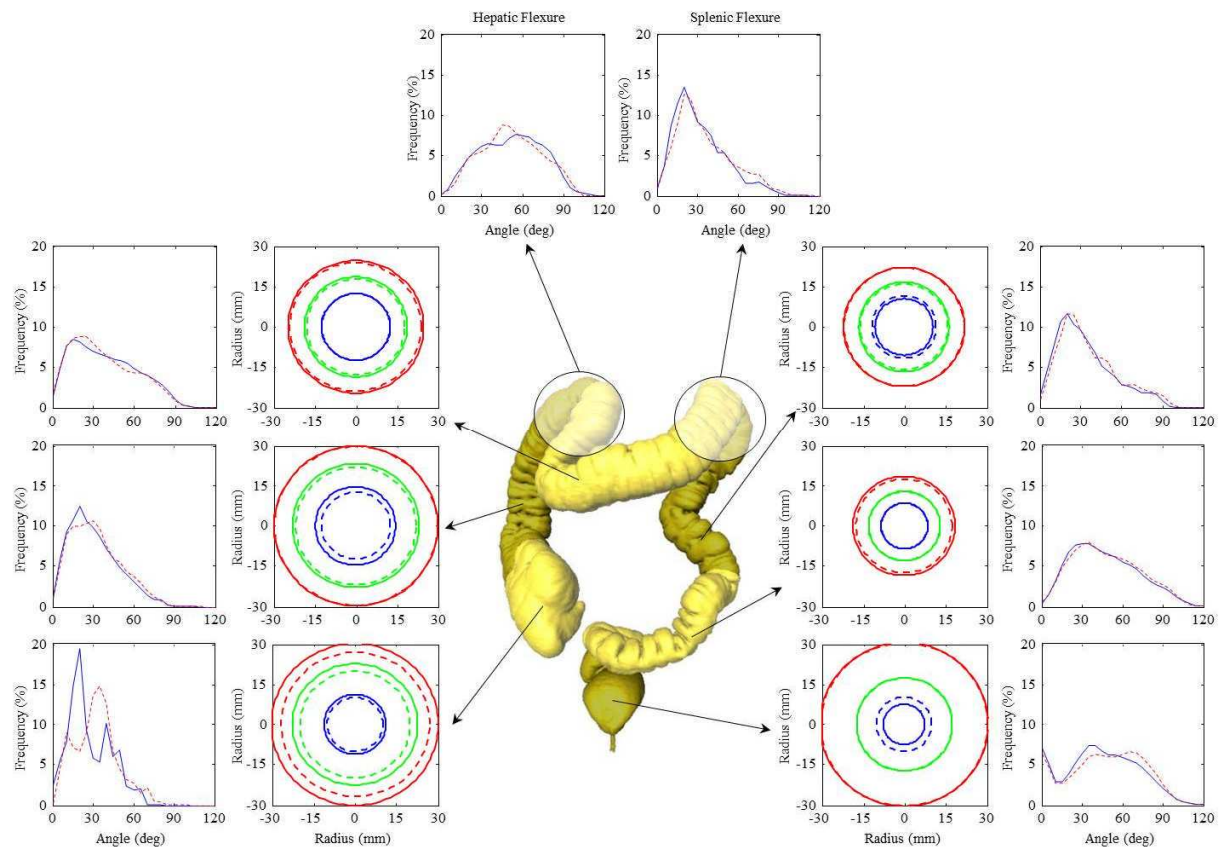
229 * Statistically Significant

230

231 Table 4. Comparison of the colonic segmental angle (mean \pm SD (median)), skewness (*s*), and
 232 kurtosis (*k*) in supine and prone orientations

	Supine		Prone	
	Angle, deg	Skew (<i>k</i>)	Angle, deg	Skew
Rectum	42.2 \pm 27.3 (42.2)	0.03 (-0.84)	45.2 \pm 28.1 (47.1)	-0.17 (-0.98)
Sigmoid	46.9 \pm 24.2 (43.8)	0.44 (-0.58)	47.9 \pm 24.1 (45.1)	0.34 (-0.71)
Descending	33.6 \pm 21.1 (29.1)	0.84 (0.07)	36.1 \pm 21.7 (31.0)	0.79 (-0.12)
Transverse	38.7 \pm 23.3 (35.6)	0.42 (-0.80)	37.2 \pm 22.9 (33.0)	0.51 (-0.69)
Ascending	30.2 \pm 17.7 (27.1)	0.69 (-0.09)	31.8 \pm 18.0 (29.7)	0.56 (-0.34)
Cecum	27.1 \pm 15.5 (22.4)	0.54 (-0.49)	32.4 \pm 15.9 (31.9)	0.42 (0.02)
Splenic *	31.5 \pm 18.5 (27.4)	0.84 (0.25)	35.1 \pm 20.4 (30.3)	0.74 (-0.17)
Hepatic *	51.8 \pm 22.4 (52.5)	0.00 (-0.82)	51.6 \pm 21.8 (50.8)	0.06 (-0.75)

233 * Artificially created segments defined around the splenic and hepatic flexures with a total length of
 234 10 cm per segment



235

236 **Fig. 5.** The 5th (blue), 50th (green), and 95th (red) percentiles of the colorectal radius and the angle
 237 frequency distributions for individual colonic segments in supine and prone orientations; **Dashed-lines**
 238 **represent prone orientation.**

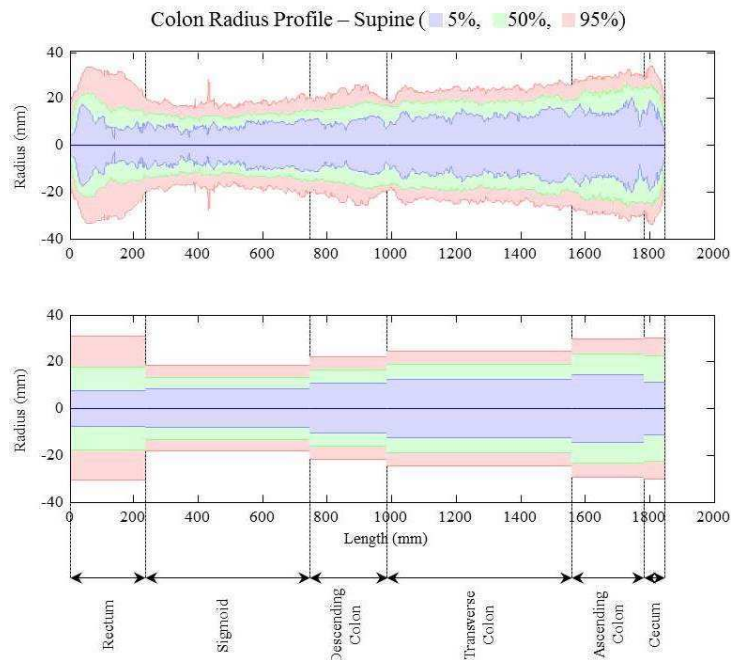
239

240 Across the colon as a whole, the total mean diameter was significantly larger in the supine position
 241 ($z=-4.29$, $p<0.01$), demonstrated mainly in the significant difference between distal colons in two
 242 different orientations ($z=-4.29$, $p<0.01$). There was no significant difference observed between the
 243 diameter of individual segments in the distal colon, however, all individual proximal segments
 244 showed significant decrease in diameter when body orientation was changed to prone (cecum: $z=-$
 245 3.19 , $p<0.01$; ascending: $z=-2.36$, $p<0.02$; and transverse: $z=-2.03$, $p<0.04$). The diameter of the other
 246 segments (distal portion) did not significantly differ between the two groups. **The diameter of the**
 247 **proximal colon was larger in men than in women, whilst that of the distal colon was larger in women.**
 248 **All other comparisons between the two gender groups yielded non-significant changes for the**
 249 **diameter variations.**

250 The total luminal volume of the colon was 1376.8 ± 582.4 cm³ in the supine position. This
 251 measure was significantly larger in the proximal colon, with its biggest portion in the transverse colon
 252 (477.9 cm³). Changing the body orientation to prone did not vary the total volume significantly
 253 (1239.5 ± 344.0 cm³). However, when individual segmental volume was compared between the two
 254 groups, the two most proximal segments were significantly smaller (cecum: $z=-2.23$, $p<0.02$ and
 255 ascending: $z=-2.91$, $p<0.01$) in the prone orientation. **When individual segmental volume was**
 256 **compared between men and women, the cecum volume was significantly larger in men in both**
 257 **orientations (supine: $p<0.013$ and prone: $p<0.028$), and the descending colon was significantly shorter**
 258 **in women (supine: $p<0.038$ and prone: $p<0.005$). All other segmental comparisons showed non-**
 259 **significant changes.**

260 Assessment of colonic segmental tortuosity is achieved using a kernel density estimation to
 261 represent the segmental angle distribution, shown in Fig. 5 with the associated skewness (s) and
 262 kurtosis (k) parameters in Table 4. Prone data showed to be less skewed (more torturous) than the
 263 supine orientation in all segments except the transverse colon. In both orientations, the descending
 264 colon has the most skewed distribution (supine: $s=0.84$ and prone: $s=0.79$) closely followed by the

265 ascending colon. Interestingly, the ascending and descending segments are held in place along their
 266 length by the colonic mesentery and considered to be less mobile than the transverse segment (which
 267 is much less constrained). The hepatic flexure exhibited a more normally distributed behavior (supine:
 268 $s=0$ and prone: $s=0.06$) when compared with the splenic flexure (supine: $s=0.84$ and prone: $s=0.74$).
 269 Data from the cecum were considered to be both less reliable and less relevant due to the segment's
 270 short length.



271
 272 Fig. 6. Two-dimensional visualisation of a segmented colon after total and segmental length
 273 normalisation; the colon centreline is laid flat and the diameter is shown as a shaded profile (for 5th,
 274 50th, and 95th percentiles) with anatomical landmarks.

275 4 Discussion

276 Colonoscopy is considered the gold standard for endoscopic examination of the whole colon.
 277 However, it is still difficult to perform or complete, mainly due to the complex colonic anatomy. In
 278 this study, we have reported a method, based purely on CTC data, to quantitatively describe the
 279 complex morphology of the colon in terms of length, diameter, volume, and tortuosity. We have
 280 examined these data across the total colon and in more detail within individual anatomical segments.
 281 These data are intended to increase our understanding of this organ and thereby help the design of
 282 future colonoscopy technology to accommodate the wide inter and intra-colon variations shown in
 283 this study.

284 The mean total colonic length in this study averaged 185.0 cm in the supine orientation and 183.0
 285 cm in the prone orientation. These are in close agreement with those found in the previous CTC study
 286 [20], however, they are significantly greater than the average reported in barium enema (up to 157 cm,
 287 for patient age range of 14-92 years) [15, 17] and in intraoperative studies (114 cm, for patient age
 288 range of 19-85 years) [18]. This discrepancy is likely to be a consequence of the population's age
 289 range and also the two-dimensional nature of these studies. Furthermore, it is possible that insufflation
 290 of the colon during CTC increases the length when compared to these studies.

291 This study demonstrates that the colonic segmental diameter changes from supine to prone
 292 orientation are influenced predominantly by intra-abdominal compression and pelvic motion. In a
 293 distended colon, the morphology of the majority of the colon is dictated primarily by changes in
 294 compressive effects, rather than by the effect of gravity. Our findings suggest that the prone position
 295 showed a higher frequency of high angles and consequently found to be more torturous than the
 296 supine position. We concluded that from these findings it would be beneficial to start device
 297 intubation in a prone position (for better rectal extension) and successively move the patient to the

298 supine position for maximum extension of the ascending colon and cecum during the colonoscopy
299 procedure.

300 The descriptive metrics generated here agree with clinical reports of colonoscopy. The sigmoid
301 colon is typically considered to be a challenging segment and our metrics reveal this segment has the
302 smallest diameter but the second longest length. The angle distribution of this segment was also
303 negatively skewed (i.e. higher tortuosity), helping to explain the reported occurrences of loop
304 formation, difficulty in passing the colonoscope, and patient discomfort during intubation found in
305 this segment [16, 30]. Normal adult human colons show considerable variations in length, radius, and
306 volume which would naturally modify the tortuosity of the colonic lumen. These factors along with
307 the pushing action exerted by the endoscopist during intubation and also the rigidity in the pushing
308 direction of the traditional colonoscope may contribute to excessive stress and stretch of bowel and
309 mesenteries, and ultimately pain felt by the patient during an uncomfortable procedure.

310 **The segmental diameters and lengths are very precious data for designers of robotic colonoscopies.**
311 **This study also defines a standardised metric that can be used to compare the tortuosity of colons**
312 **between subjects and body orientations. Although the angle or tortuosity of the colon can be changed**
313 **under the pressure exerted by the scope or even body orientation, but it remains an important metric**
314 **when designing a contactless robotic platforms or even atraumatic scopes. An example of this is**
315 **swimming or magnetic capsules, which are under development, and don't rely on contact with colonic**
316 **wall for their locomotion strategies. Our findings will help the community to optimise the length,**
317 **diameter, and articulation parameters of new robotic platforms for an improved navigation and**
318 **locomotion strategies.**

319 The geometry of colonoscopy devices (notably their diameter, segmental length and articulation
320 range) are necessarily constrained and defined by the luminal environment of the colon. It is essential
321 that they are appropriately designed such that they can move within the torturous lumen without
322 imposing excessive force on the tissue (risking discomfort or colon damage) and support functionality
323 to image or take biopsies. Considering the conceptual design of a robotic system for colonoscopy
324 requires guidance on factors such as the device diameter and ability to articulate. Referring to Fig. 5
325 and 6, it is evident that the rigid diameter of the robot should not be greater than 17 mm which is the
326 5th percentile of the sigmoid colon (the Olympus CF-140L adult video colonoscope features a 12.9
327 mm outer diameter tube). Furthermore, the body of the robot must be flexible enough, or articulate, to
328 conform to the acute bends shown in Fig. 2. a significant number of which are $>90^\circ$. We used a span
329 size of 35 mm (which is the equivalent of total colonic average diameter in prone position) to analyze
330 the in-plane angle of the lumen centerline but this could readily be adapted for devices of different
331 lengths.

332 The results from this study give the research community a dataset defining engineering
333 requirements for the design of colonoscopy devices. Furthermore, it provides a robust methodology
334 with which to obtain these metrics. Thus the preliminary dataset presented here can be readily
335 extended with complementary information and extended to cover different populations, age groups
336 and disease types, helping to ensure that future colonoscopy systems are best designed to meet their
337 clinical need.

338 **5 Acknowledgements**

339 Competing interests: None declared

340 Funding: This work was supported by the ERC under project reference 268519.

341 Ethical approval: Not required

342 **6 References**

343 [1] CRUK.(March2014).Available:<http://info.cancerresearchuk.org/cancerstats>.

344 [2] NCI.(March2014).Available:<http://www.cancer.gov/cancertopics>.

- 345 [3] Baxter NN, Goldwasser MA, Paszat LF, Saskin R, Urbach DR, Rabeneck L. Association
346 of colonoscopy and death from colorectal cancer. *Ann Intern Med.* 2009;150:1-8.
- 347 [4] Force USPST. Screening for Colorectal Cancer: U.S. Preventive Services Task Force
348 Recommendation Statement. *Annals of Internal Medicine.* 2008;149:627.
- 349 [5] Cotton PB, Durkalski VL, Pineau BC, Palesch YY, Mauldin PD, Hoffman B, et al.
350 Computed tomographic colonography (virtual colonoscopy): a multicenter comparison with
351 standard colonoscopy for detection of colorectal neoplasia. *JAMA.* 2004;291:1713-9.
- 352 [6] Eickhoff A, Van Dam J, Jakobs R, Kudis V, Hartmann D, Damian U, et al. Computer-
353 assisted colonoscopy (The NeoGuide Endoscopy System): Results of the first human clinical
354 trial ("PACE study"). *Am J Gastroenterol.* 2007;102:261-6.
- 355 [7] Vucelic B, Rex D, Pulanic R, Pfefer J, Hrstic I, Levin B, et al. The aer-o-scope: proof of
356 concept of a pneumatic, skill-independent, self-propelling, self-navigating colonoscope.
357 *Gastroenterology.* 2006;130:672-7.
- 358 [8] Cosentino F, Tumino E, Passoni GR, Morandi E, Capria A. Functional evaluation of the
359 endotics system, a new disposable self-propelled robotic colonoscope: in vitro tests and
360 clinical trial. *Int J Artif Organs.* 2009;32:517-27.
- 361 [9] Shike M, Fireman Z, Eliakim R, Segol O, Sloyer A, Cohen LB, et al. Sightline ColonoSight
362 system for a disposable, power-assisted, non-fiber-optic colonoscopy (with video).
363 *Gastrointest Endosc.* 2008;68:701-10.
- 364 [10] Rosch T, Adler A, Pohl H, Wettschureck E, Koch M, Wiedenmann B, et al. A motor-
365 driven single-use colonoscope controlled with a hand-held device: a feasibility study in
366 volunteers. *Gastrointest Endosc.* 2008;67:1139-46.
- 367 [11] Valdastrì P, Quaglia C, Susilo E, Menciassi A, Dario P, Ho CN, et al. Wireless
368 therapeutic endoscopic capsule: in vivo experiment. *Endoscopy.* 2008;40:979-82.
- 369 [12] Tortora G, Valdastrì P, Susilo E, Menciassi A, Dario P, Rieber F, et al. Propeller-based
370 wireless device for active capsular endoscopy in the gastric district. *Minim Invasive Ther*
371 *Allied Technol.* 2009;18:280-90.
- 372 [13] Valdastrì P, Ciuti G, Verbeni A, Menciassi A, Dario P, Arezzo A, et al. Magnetic air
373 capsule robotic system: proof of concept of a novel approach for painless colonoscopy. *Surg*
374 *Endosc.* 2012;26:1238-46.
- 375 [14] Dafnis G, Granath F, Pahlman L, Ekblom A, Blomqvist P. Patient factors influencing the
376 completion rate in colonoscopy. *Dig Liver Dis.* 2005;37:113-8.
- 377 [15] Sadahiro S, Ohmura T, Yamada Y, Saito T, Taki Y. Analysis of Length and Surface-
378 Area of Each Segment of the Large-Intestine According to Age, Sex and Physique. *Surgical*
379 *and Radiologic Anatomy.* 1992;14:251-7.
- 380 [16] Saunders BP, Fukumoto M, Halligan S, Jobling C, Moussa ME, Bartram CI, et al. Why is
381 colonoscopy more difficult in women? *Gastrointestinal Endoscopy.* 1996;43:124-6.
- 382 [17] Saunders BP, Halligan S, Jobling C, Fukumoto M, Moussa ME, Williams CB, et al. Can
383 barium enema indicate when colonoscopy will be difficult? *Clinical Radiology.* 1995;50:318-
384 21.
- 385 [18] Saunders BP, Phillips RK, Williams CB. Intraoperative measurement of colonic anatomy
386 and attachments with relevance to colonoscopy. *Br J Surg.* 1995;82:1491-3.
- 387 [19] Hounnou G, Destrieux C, Desme J, Bertrand P, Velut S. Anatomical study of the length
388 of the human intestine. *Surg Radiol Anat.* 2002;24:290-4.
- 389 [20] Punwani S, Halligan S, Tolan D, Taylor SA, Hawkes D. Quantitative assessment of
390 colonic movement between prone and supine patient positions during CT colonography.
391 *British Journal of Radiology.* 2009;82:475-81.

- 392 [21] Khashab MA, Pickhardt PJ, Kim DH, Rex DK. Colorectal anatomy in adults at computed
393 tomography colonography: normal distribution and the effect of age, sex, and body mass
394 index. *Endoscopy*. 2009;41:674-8.
- 395 [22] Eickhoff A, Pickhardt PJ, Hartmann D, Riemann JF. Colon anatomy based on CT
396 colonography and fluoroscopy: impact on looping, straightening and ancillary manoeuvres in
397 colonoscopy. *Dig Liver Dis*. 2010;42:291-6.
- 398 [23] Hanson ME, Pickhardt PJ, Kim DH, Pfau PR. Anatomic Factors Predictive of Incomplete
399 Colonoscopy Based on Findings at CT Colonograph. *American Journal of Roentgenology*.
400 2007;189:774-9.
- 401 [24] Obstein KL, Valdastrì P. Advanced endoscopic technologies for colorectal cancer
402 screening. *World Journal of Gastroenterology : WJG*. 2013;19:431-9.
- 403 [25] National Ct Colonography Trial. American College of Radiology Imaging Network,
404 ACRIN 66642004.
- 405 [26] Wyatt CL, Ge Y, Vining DJ. Automatic segmentation of the colon for virtual colonoscopy.
406 *Comput Med Imaging Graph*. 2000;24:1-9.
- 407 [27] Ingmar B. Penalized-Distance Volumetric Skeleton Algorithm. *IEEE Transactions on*
408 *Visualization and Computer Graphics*. 2001;7:195-206.
- 409 [28] Ge Y, Stelts DR, Wang J, Vining DJ. Computing the centerline of a colon: a robust and
410 efficient method based on 3D skeletons. *J Comput Assist Tomogr*. 1999;23:786-94.
- 411 [29] Taylor S, Halligan S, Goh V, Morley S, Bassett P, Atkin W. Optimizing colonic distention
412 for multi-detector row CT colonography: effect of hyoscine butylbromide and rectal balloon
413 catheter. *Radiology*. 2003;229:99-108.